ARTICLES

Proposed differential-frequency-readout system by hysteretic Josephson junctions

L. Z. Wang
Department of Physics and Astronomy, University of New Mexico, Albuquerque, New Mexico 87131

Robert V. Duncan
Sandia National Laboratories, Albuquerque, New Mexico 87185
and Department of Physics and Astronomy, University of New Mexico, Albuquerque, New Mexico 87131
(Received 22 November 1991)

The Josephson relation $V=nh\nu/2e$ has been verified experimentally to 3 parts in 10^{19} [A. K. Jain, J. E. Lukens, and J.-S. Tsai, Phys. Rev. Lett. **58**, 1165 (1987)]. Motivated by this result, we propose a differential-frequency-readout system by two sets of hysteretic Josephson junctions rf biased at millimeter wavelengths. Because of the Josephson relation, the proposed differential-frequency-readout system is not limited by photon fluctuation, which limits most photon-detection schemes. In the context of the Stewart-McCumber model [W. C. Stewart, Appl. Phys. Lett. **12**, 277 (1968); D. E. McCumber, J. Appl. Phys. **39**, 3113 (1968)] of Josephson junctions, we show theoretically that the differential frequency of the two milliwave biases can be read out by the proposed system to unprecedented accuracy. The stability of the readout scheme is also discussed. The measurement uncertainty of the readout system resulting from the intrinsic thermal noise in the hysteretic junctions is shown to be insignificant. The study of two single junctions can be extended to two sets of Josephson junctions connected in series (series array) in this measurement scheme provided that junctions are separated by at least 10 μm [D. W. Jillie, J. E. Lukens, and Y. H. Kao, Phys. Rev. Lett. **38**, 915 (1977)]. The sensitivity for the differential frequency detection may be increased by biasing both series arrays to a higher constant-voltage step.

PACS number(s): 06.20.−f, 07.62.+s, 85.25.−j

I. INTRODUCTION

The Josephson voltage-frequency relation has been confirmed to be the same within two different Josephson junctions to an ultrahigh accuracy [1]. In such experiments [1,3–6], two Josephson junctions in series opposition are biased on the nth microwave-induced voltage step with the same microwave source. Any dc voltage difference between the two Josephson junctions will create a current within the superconductive coil connecting them. This current can be measured by coupling the magnetic flux generated by the coil into a superconducting quantum interference device (SQUID) magnetometer. The null result [1] obtained by one of these experiments indicates that the Josephson relation $V=nh\nu/2e$ differs by no more than 3 parts in 10^{19}, where V is the dc voltage of the junction, n is an integer, h is Planck's constant, ν is the frequency of the microwave bias, and e is the elementary electric charge. The profound impact of this measurement technology on our understanding of fundamental physics has been reviewed by McDonald [7].

This unprecedented accuracy has motivated us to propose an interferometric readout at millimeter wavelengths [8]. In brief, the system consists of two sets of Josephson-junction arrays biased by two different microwave frequencies generated by an active interferometer [9]. The differential frequency of the interferometer can be measured by the scheme described above and diagrammed in Fig. 1. If the highly accurate results of the previous null experiments [1,3–6] were due to the rigidity of the superconductor, the proposed new interferometric readout scheme could have failed to respond to the small frequency difference. However, Bracken and Hamilton [4] have used different frequency microwaves to bias each individual junction. They have reported the linear relation between the frequency difference and the voltage difference of two Josephson junctions and achieved an accuracy of $\Delta V/V \leq 5\times 10^{-9}$. Since then the realization of this kind of scheme has not been clarified. A question concerning the intrinsic limit due to the thermal noise in the junctions still remains unanswered. In this paper we theoretically analyze in detail the system of two hysteretic junctions according to the Stewart-McCumber model [2]. In the following section, we will show that the dc voltage difference between two junctions which are both locked on the nth voltage step does indeed respond linearly to the difference of the two microwave bias frequencies. The theoretical implication of a comparison of microwave-induced constant-voltage steps in Josephson junctions with the same microwave source is also addressed in this section. In Sec. III we consider the stability of the scheme when it is biased by two different microwave frequencies on the same integer step. The response time to detect a change in the differential fre-

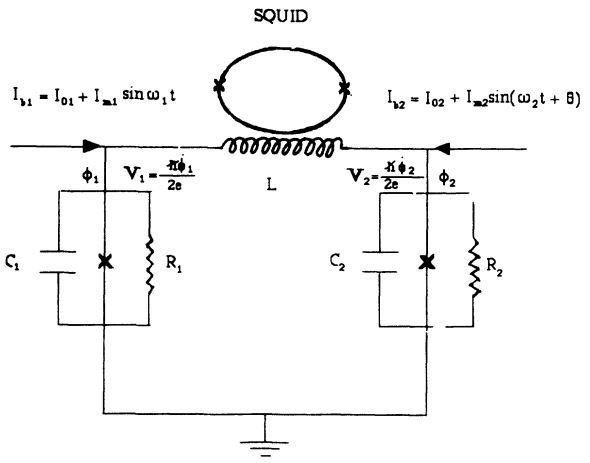

FIG. 1. The schematic circuit for the differential-frequency-readout system.

quency of the microwave biases is estimated by using realistic junction parameters and coupling inductance. The intrinsic uncertainty of this measurement scheme is mainly due to the thermal noise at the junctions. In Sec. IV we have derived a Fokker-Planck equation for two junctions with Johnson noise which comes from the quasiparticle current tunneling in each junction. The voltage roundoff due to the fluctuation of the dc bias current for each junction at nonzero temperature can be analyzed according to these equations. With a real measurement situation and with the previous results obtained by Biswas and Jha [10] for a single junction, the measurement uncertainty of this scheme due to the thermal junction noise has been estimated. The optimized operation for this measurement scheme is described in this section as well. Finally, Sec. V contains our summary and conclusion.

II. MODEL FOR THE MEASUREMENT SCHEME

The Stewart-McCumber model [2] for our system is shown in Fig. 1. It consists of two ideal Josephson elements with critical current I_{ci} shunted by a resistance R_i and a capacitance c_i, and driven by a current source I_{bi} for each junction $i=1,2$. The inductance L between two junctions generates magnetic flux due to the voltage difference between the two junctions. The junction voltage V_i and phase ϕ_i obey the following differential equations:

$$\frac{\hbar c_1}{2e}\ddot{\phi}_1+\frac{\hbar}{2eR_1}\dot{\phi}_1+I_{c1}\sin\phi_1=I_{b1}+\frac{\hbar}{2eL}\int_0^t(\dot{\phi}_2-\dot{\phi}_1)dt \ , \tag{2.1}$$

$$\frac{\hbar c_2}{2e}\ddot{\phi}_2+\frac{\hbar}{2eR_2}\dot{\phi}_2+I_{c2}\sin\phi_2=I_{b2}+\frac{\hbar}{2eL}\int_0^t(\dot{\phi}_1-\dot{\phi}_2)dt \ , \tag{2.2}$$

and

$$V_i=\frac{\hbar\dot{\phi}_i}{2e} \quad \text{for each } i=1,2 \ .$$

The bias currents can be written by

$$I_{b1}=I_{01}+I_{m1}\sin\omega_1 t \ , \tag{2.3}$$

$$I_{b2}=I_{02}+I_{m2}\sin(\omega_2 t+\theta) \ , \tag{2.4}$$

where I_{0i} and I_{mi} are the dc current bias and the microwave current amplitude, respectively, and θ is the relative phase between two microwave sources. Equations (2.1)–(2.4) are our basic equations for this readout scheme.

To solve Eqs. (2.1) and (2.2) analytically, we consider a hysteretic junction whose parameters are in region I in Fig. 2 of Kautz's paper [11]. In this junction parameter region we have $R_i>\omega_i L_i>1/\omega_i c_i$, where $L_i=\hbar/2eI_{ci}$ is the Josephson inductance for each junction. Therefore most of the microwave current flows through the junctions' capacitive reactances. For experimental interest, the impedance between the two junctions at microwave radiation frequencies is large compared with the individual junction impedances (the inductance between two junctions, $L\approx\mu$H–nH; the junction capacitance, $c_i\approx 100-10$ pF, the junction resistance, $R_i\approx 1-100\ \Omega$, and the junction critical current, $I_{ci}\approx 10-1000\ \mu$A, for a hysteretic junction; the biased microwave frequency is about 100 GHz [12]). That is, $\omega_i L\gg Z_i$ for $i=1,2$, where ω_i and Z_i are the microwave angular frequency and impedance for the ith junction. The circuit between the two junctions is approximately open at the biasing microwave frequencies. Thus the microwave bias for each junction can be considered to be approximately independent. We have the following approximation for each junction [12,31]:

$$\frac{\hbar c_i}{2e}\ddot{\phi}_i\approx I_{mi}\sin(\omega_i t+\theta_i) \ , \tag{2.5}$$

where

$$\theta_i=0 \quad \text{for } i=1 \quad \text{and} \quad \theta_i=\theta \quad \text{for } i=2 \ .$$

After a simple integration, one has

$$\dot{\phi}_i\approx\dot{\phi}_{0i}-\frac{2eI_{mi}}{\hbar c_i\omega}\cos(\omega_i t+\theta_i) \tag{2.6}$$

and

$$\phi_i\approx\phi_{0i}+\dot{\phi}_{0i}t-\frac{2eI_{mi}}{\hbar c_i\omega_i^2}\sin(\omega_i t+\theta_i) \ . \tag{2.7}$$

Substituting Eqs. (2.5), (2.6), and (2.7) into Eqs. (2.1) and (2.2), we obtain

$$\frac{\hbar}{2eR_1}\left[\dot{\phi}_{01}-\frac{2eI_{m1}}{\hbar c_1\omega_1}\cos\omega_1 t\right]+I_{c1}\sum_{n=-\infty}^{\infty}J_n\left[\frac{2eI_{m1}}{\hbar c_1\omega_1^2}\right]\sin[\phi_{01}+(\dot{\phi}_{01}-n\omega_1)t]$$
$$=I_{01}+\frac{\hbar}{2eL}\int_0^t\left[\dot{\phi}_{02}-\dot{\phi}_{01}-\frac{2eI_{m2}}{\hbar c_2\omega_2}\cos(\omega_2 t'+\theta)+\frac{2eI_{m1}}{\hbar c_1\omega_1}\cos\omega_1 t'\right]dt' , \quad (2.8)$$

$$\frac{\hbar}{2eR_2}\left[\dot{\phi}_{02}-\frac{2eI_{m2}}{\hbar c_2\omega_2}\cos(\omega_2 t+\theta)\right]+I_{c2}\sum_{n=-\infty}^{\infty}J_n\left[\frac{2eI_{m2}}{\hbar c_2\omega_2^2}\right]\sin[\phi_{02}-n\theta+(\dot{\phi}_{02}-n\omega_2)t]$$
$$=I_{02}+\frac{\hbar}{2eL}\int_0^t\left[\dot{\phi}_{01}-\dot{\phi}_{02}-\frac{2eI_{m1}}{\hbar c_1\omega_1}\cos\omega_1 t'+\frac{2eI_{m2}}{\hbar c_2\omega_2}\cos(\omega_2 t'+\theta)\right]dt' . \quad (2.9)$$

Here we have used the well-known relation

$$\sin\left[\phi_{0i}+\dot{\phi}_{0i}t\frac{2eI_{mi}}{\hbar c_i\omega_i^2}\sin(\omega_i t+\theta_i)\right]$$
$$=\sum_{n=-\infty}^{\infty}J_n\left[\frac{2eI_{mi}}{\hbar c_i\omega_i^2}\right]\sin[\phi_{0i}-n\theta_i+(\dot{\phi}_i-n\omega_i)t] ,$$

and $J_n(x)$ is the nth-order Bessel function. Taking the time average and assuming that both junctions are locked on the same integer step n, we obtain

$$\frac{\hbar}{2eR_1}\dot{\phi}_{01}+I_{c1}J_n\left[\frac{2eI_{m1}}{\hbar c_1\omega_1^2}\right]\sin\phi_{01}$$
$$=I_{01}+\frac{\hbar}{2eL}\int_0^t(\dot{\phi}_{02}-\dot{\phi}_{01})dt' , \quad (2.10)$$

$$\frac{\hbar}{2eR_2}\dot{\phi}_{02}+I_{c2}J_n\left[\frac{2eI_{m2}}{\hbar c_2\omega_2^2}\right]\sin(\phi_{02}+n\theta)$$
$$=I_{02}+\frac{\hbar}{2eL}\int_0^t(\dot{\phi}_{01}-\dot{\phi}_{02})dt' , \quad (2.11)$$

$\dot{\phi}_{01}=n\omega_1$ and $\dot{\phi}_{02}=n\omega_2$.

That is,

$$I_{01}=\frac{n\hbar\omega_1}{2eR_1}+I_{c1}J_n\left[\frac{2eI_{m1}}{\hbar c_1\omega_1^2}\right]\sin\phi_{01}+\frac{n\hbar}{2eL}\int_0^t(\omega_1-\omega_2)dt' , \quad (2.12)$$

$$I_{02}=\frac{n\hbar\omega_2}{2eR_2}+I_{c2}J_n\left[\frac{2eI_{m2}}{\hbar c_2\omega_2^2}\right]\sin(\phi_{02}+n\theta)$$
$$+\frac{n\hbar}{2eL}\int_0^t(\omega_2-\omega_1)dt' . \quad (2.13)$$

From Eqs. (2.12) and (2.13), we clearly see that if both junctions are locked on the same integer step n, there is a current in the third term of each equation [Eqs. (2.12) and (2.13)] linearly proportional to the difference of the two microwave frequencies with opposite sign. This current comes from the dc voltage difference between the two junctions. Accordingly, the magnetic flux generated in the inductance between two junctions is

$$\Phi=\frac{nh}{2e}\int_0^t(\nu_1-\nu_2)dt' , \quad (2.14)$$

which may be measured by a SQUID magnetometer, where $\nu_i=\omega_i/2\pi$ is the microwave frequency. We also notice that Eq. (2.14) depends only on the physical constant $nh/2e$, that is, a number n of fundamental units of flux (fluxons). The magnetic flux resolution of a typical SQUID is about $10^{-5}h/2e$ per $\sqrt{\text{Hz}}$. Thus, provided that no other noises are significant, the resolution of the frequency difference is

$$\delta(\Delta\nu)=10^{-5}/n(\Delta t)^{3/2}\ \text{Hz} , \quad (2.15)$$

where Δt is the measurement time in seconds. According to Eq. (2.15) we see that the resolution of the differential frequency is proportional to the quantum number n. This is because the phase of the Josephson junction oscillates n periods during one microwave period on the phase-locked state and the phase differences of two Josephson junctions have been compared by detecting the magnetic flux in the inductance. Thus the differential frequency of the microwaves is resolved by the relation between the phase difference of the Josephson junctions and the phase difference of the two microwave signals during a measurement time. Notice that the resolution of the differential frequency is proportional to $(\Delta t)^{3/2}$. The power of $\frac{3}{2}$ of the measurement time results from the fact that the number of periods read by the scheme is proportional to the measurement time and thus the phase difference of the two microwave sources is linearly proportional to the measurement time; and an addition $\frac{1}{2}$ power of the measurement period results from the SQUID noise.

Finally, we shall discuss the theoretical implication of comparisons [1,3–6] of microwave-induced constant-voltage steps in Josephson junctions. There have been a number of discussions on the validity of the Josephson voltage-frequency relationship ($V_n=n\hbar\nu/2e$). This relationship has been shown to be independent (to a high degree) of both the types and the materials of the links and superconductors comprising the junction. However, several authors [13,14] have proposed possible corrections to the Josephson voltage-frequency relation. It has been argued on very fundamental grounds that the ac Josephson relation must be exact [15,16]. Thus any evidence that the Josephson relation is not identical for all types of Josephson junctions could cause a fundamental change in our understanding of their behavior. If the ac Josephson relationship is not universal, then

$$V_n=K(nh/2e)\nu , \quad (2.16)$$

where K could not be a universal constant ($K \neq 1$). That is, we replace $h/2e$ by $K_i h/2e$ in Eqs. (2.1) and (2.2). Suppose that we bias two Josephson junctions on the same integer step n with the same microwave frequency. Then following the same analysis above, the voltage difference between two junctions would be

$$\Delta V_n = (K_1 - K_2)(nh/2e)\nu = \Delta K V_n \ . \tag{2.17}$$

Thus from the best result obtained by Jain, Lukens, and Tsai [1], ΔK is no more than 3 parts in 10^{19}.

III. THE STABILITY OF THE MEASUREMENT SCHEME

The stability for a single hysteric junction on a phase-locked state has been studied by Kautz [11,17]. However, because of the nonlinear nature of the Josephson junction, the scheme considered here is not obviously stable during its operation. That is, the inductance coupling the two junctions may induce an instability for both phase-locked junctions. We shall now examine the stability for this scheme in detail.

The local stability in the presence of infinitesimal perturbations is determined by the largest Liapunov exponent. When the largest Liapunov exponent is negative, all small perturbations will decay and the system will return to the same phase-locked state. If the largest Liapunov exponent is positive, then the system wanders away from the original phase-locked state and will either reach a new phase-locked state or go into a chaotic state.

We begin our approach by defining

$$\phi = \phi_{ip} + \delta_i \quad \text{for each } i = 1,2 \ , \tag{3.1}$$

where ϕ_{ip} is the phase of the phase-locked state, and δ_i is the infinitesimal perturbation. Introducing Eq. (3.1) into Eqs. (2.1) and (2.2), one obtains

$$\frac{\hbar c_1}{2e}\ddot{\delta}_1 + \frac{\hbar}{2eR_1}\dot{\delta}_1 + I_{c1}\cos\phi_{1p}\delta_1 = \frac{\hbar}{2eL}(\delta_2 - \delta_1) - \frac{\hbar}{2eL}\Delta\delta(0) \ , \tag{3.2}$$

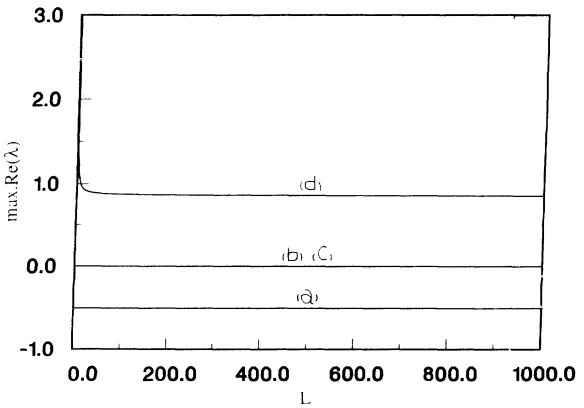

FIG. 2. The largest real part of the Liapunov exponent (in units of $1/RC$) vs the coupling inductance L (in units of L'_{Ji}) for (a) $L'_{Ji} = 100$ pH, (b) $L'_{Ji} = 10^{10}$ H, (c) $L'_{Ji} = -10^{10}$ H, (d) $L'_{Ji} = -10$ nH with $R_i = 40\ \Omega$ and $C_i = 100$ pF.

$$\frac{\hbar c_1}{2e}\ddot{\delta}_2 + \frac{\hbar}{2eR_2}\dot{\delta}_2 + I_{c2}\cos\phi_{2p}\delta_2 = \frac{\hbar}{2eL}(\delta_1 - \delta_2) + \frac{\hbar}{2eL}\Delta\delta(0) \ , \tag{3.3}$$

where $\Delta\delta(0) = \delta_2(0) - \delta_1(0)$. Here we have made a linear approximation for δ_i. Since both junctions are hysteretic, $\cos\phi_{ip}$ can be replaced by the time average $\langle \cos\phi_{ip} \rangle$ [11]. To solve Eqs. (3.2) and (3.3), we transform into four coupled first-order linear differential equations:

$$\frac{\partial}{\partial t}\begin{bmatrix} \dot{\delta}_1 \\ \delta_1 \\ \dot{\delta}_2 \\ \delta_2 \end{bmatrix} = \begin{bmatrix} \frac{-1}{R_1 c_1} & -K_1 & 0 & \frac{1}{Lc_1} \\ 1 & 0 & 0 & 0 \\ 0 & \frac{1}{Lc_2} & \frac{-1}{R_2 c_2} & -K_2 \\ 0 & 0 & 1 & 0 \end{bmatrix} \begin{bmatrix} \dot{\delta}_1 \\ \delta_1 \\ \dot{\delta}_2 \\ \delta_2 \end{bmatrix} + \begin{bmatrix} \frac{-\Delta\delta(0)}{Lc_1} \\ 0 \\ \frac{\Delta\delta(0)}{Lc_2} \\ 0 \end{bmatrix} , \tag{3.4}$$

where

$$K_i = \frac{2eI_{ci}\langle \cos\phi_{ip} \rangle}{hc_i} + \frac{1}{Lc_i} = \frac{1}{c_i}\left[\frac{1}{L'_{Ji}} + \frac{1}{L}\right] \quad \text{for } i = 1,2 \ ; \tag{3.5}$$

here $L'_{Ji} = h/2eI_{ci}\langle \cos\phi_{ip} \rangle$ is the generalized Josephson inductance. We study the eigenvalues of Eqs. (3.4) and (3.5) numerically with the parameter range $R_i \approx 100$–$1\ \Omega$, $C_i \approx 100$–1 pF, $L_{Ji} \approx \pm 100$–± 1 pH. We found that the sign of the largest real part of the Liapunov exponent strongly depends on the sign of L'_{Ji}. The largest real part of the Liapunov exponent is independent of the coupling inductance, when $L \geq L'_{Ji}$. For $L \ll L'_{Ji}$, the largest real part of the Liapunov exponent changes dramatically. However, the sign of the largest real part of the Liapunov exponent is still the same for a fixed sign of L'_{Ji}. Figure 2 shows the largest real part of the Liapunov exponent (in units of $1/RC$) versus the coupling inductance L (in units of L'_{Ji}) for (a) $L'_{Ji} = 100$ pH, (b) $L'_{Ji} = 10^{10}$ H, (c) $L'_{Ji} = -10^{10}$ H, (d) $L'_{Ji} = -10$ nH with $R_i = 40\ \Omega$ and $C_i = 100$ pF. We see that the largest real part of the Liapunov exponent changes sign from $-1/|L'_{Ji}|$ to $1/|L'_{Ji}|$.

The eigenvalues of the above matrix are the Liapunov exponents, which are the roots of the following quartic equation:

$$x^4 + \left[\frac{1}{R_1 c_1} + \frac{1}{R_2 c_2}\right]x^3 + \left[K_1 + K_2 + \frac{1}{R_1 c_1 R_2 c_2}\right]x^2 + \left[\frac{K_2}{R_1 c_1} + \frac{K_1}{R_2 c_2}\right]x + \left[K_1 K_2 - \frac{1}{c_1 c_2 L^2}\right] = 0 \ . \tag{3.6}$$

Then if the λ_i are the eigenvalues, i.e., the Liapunov exponents, we have

$$\sum_{i=1}^{4}\lambda_i=-\left[\frac{1}{R_1c_1}+\frac{1}{R_2c_2}\right] \tag{3.7}$$

and

$$\prod_{i=1}^{4}\lambda_i=K_1K_2-\frac{1}{c_1c_2L^2}\ . \tag{3.8}$$

We notice that if the generalized Josephson inductances $L'_{Ji}\geq 0$, the coefficients of the quartic equation are all greater than zero; then, the curve of Eq. (3.6) monotonically increases for $x>0$. The interceptions between Eq. (3.6) and the x axis must be on the left side of the y axis. Thus the solutions of the quartic equation must be less than zero. When $L'_{Ji}<0$, one can shift the x axis such that the new x axis intercepts the curve at the origin. One can see that there exists at least one positive interception with the old x axis. Thus the measurement scheme is unstable with a positive Liapunov exponent. This analysis is consistent with our numerical study. Since $\langle\cos\phi_{1p}\rangle$ and $\langle\cos\phi_{2p}\rangle$ are both greater than zero (provided the two junctions are independently phase locked on a stable voltage step n [11]), this measurement scheme is stable when it operates on phase-locked states initially. The stability of the two junctions will not be degraded by connecting an inductance between them. We notice from Eq. (3.7) that the sum of the Liapunov exponents equals the sum of the inverse of the junction's RC time constants. This indicates that for any small dynamic perturbation in this scheme, the relaxation time is about a junction's RC time constant [see curve (a) in Fig. 2]. Typical junction parameters used in a series array of a voltage standard are $R\sim 40\ \Omega$, $C\sim 35$ pF, and $L_{Ji}\sim 10$ pH. The system response time is on the order of a nanosecond. Thus the signal for this kind of readout system must be slower than nanoseconds. However, in a practical device the response time of a SQUID becomes the main limiting factor, with a 3-dB bandwidth of about 10 kHz.

IV. INTRINSIC NOISE

The effect of noise on the current-voltage characteristic of a Josephson junction has been investigated by a number of authors [10,11,18–22]. Since the region of junction parameters and microwave frequency of interest is far away from the chaotic regime we will not consider the noise due to the chaotic motion of the junction phase [23–29]. The intrinsic thermal noise on a rf-induced step at a dc voltage V was derived by Stephen [18]. In terms of the Steward-McCumber model Stephen's result for the two-time correlation function is

$$\langle I_N(t_1)I_N(t_2)\rangle=\frac{eV_n}{R}\coth(eV_n/2kT)\delta(t_1-t_2)\ , \tag{4.1}$$

which accounts for the shot noise associated with the quasiparticle current, where V_n is the dc voltage of the junction, k is Boltzmann's constant, and T is the ambient temperature. The assumed noise power spectrum is white as implied by the δ-function time dependence of the correlation function. Because the noise power spectrum is generally frequency dependent [30] the form used here is strictly correct only for noise frequencies less than eV_n/h. For present purposes the noise need not be accurately represented at high frequencies since the junction is insensitive to noise above the plasma frequency [11]. With noise included we rewrite Eqs. (2.1) and (2.2),

$$\frac{\hbar c_1}{2e}\ddot{\phi}_1+\frac{\hbar}{2eR_1}\dot{\phi}_1+I_{c1}\sin\phi_1 =I_{b1}+\frac{\hbar}{2eL}\int_0^t(\dot{\phi}_2-\dot{\phi}_1)dt+I_{N1}\ , \tag{4.2}$$

$$\frac{\hbar c_2}{2e}\ddot{\phi}_1+\frac{\hbar}{2eR_2}\dot{\phi}_1+I_{c2}\sin\phi_2 =I_{b2}+\frac{\hbar}{2eL}\int_0^t(\dot{\phi}_1-\dot{\phi}_2)dt+I_{N2}\ , \tag{4.3}$$

where I_{N1} and I_{N2} are Johnson noise, in the form of Eq. (4.1) for each of the two junctions. To describe the effect of thermal noise and the phase-locked state, we consider a situation in which a periodic solution ϕ_{pi} exists in the absence of noise and calculate the deviation δ_i of the phase from ϕ_{pi} in the presence of noise. Thus we consider a solution to Eqs. (4.2) and (4.3) of the form

$$\phi=\phi_{ip}+\delta_i \quad \text{for each } i=1,2\ . \tag{4.4}$$

Substituting (4.4) into Eqs. (4.2) and (4.3) and replacing $\sin\phi_{ip}$ and $\cos\phi_{ip}$ by the time average $\langle\sin\phi_{ip}\rangle$ and $\langle\cos\phi_{ip}\rangle$, and using the same argument as in Sec. III, we obtain

$$\frac{\hbar c_1}{2e}\ddot{\delta}_1+\frac{\hbar}{2eR_1}\dot{\delta}_1+I_{c1}J_n\left[\frac{2eI_{m1}}{\hbar c_1\omega_1^2}\right]\sin(\delta_1+\phi_{01}) =\Delta I_{01}+\frac{\hbar}{2eL}(\delta_2-\delta_1)-\frac{\hbar}{2eL}\Delta\delta(0)+I_{N1}\ , \tag{4.5}$$

$$\frac{\hbar c_2}{2e}\ddot{\delta}_2+\frac{\hbar}{2eR_2}\dot{\delta}_2+I_{c2}J_n\left[\frac{2eI_{m2}}{\hbar c_2\omega_2^2}\right]\sin(\delta_2+\phi_{02}+n\theta) =\Delta I_{02}+\frac{\hbar}{2eL}(\delta_1-\delta_2)+\frac{\hbar}{2eL}\Delta\delta(0)+I_{N2}\ , \tag{4.6}$$

where

$$\Delta I_{01}=I_{01}-\frac{n\hbar\omega_1}{2eR_1}-\frac{n\hbar}{2eL}\int_0^t(\omega_1-\omega_2)dt' \tag{4.7}$$

and

$$\Delta I_{02}=I_{02}-\frac{n\hbar\omega_2}{2eR_2}-\frac{n\hbar}{2eL}\int_0^t(\omega_2-\omega_1)dt'\ , \tag{4.8}$$

where ΔI_{01} and ΔI_{02} are the current deviations from the centers of the constant-voltage steps, respectively. The procedure used is similar to that in Sec. III except that here we do not make a linear approximation. We notice that Eqs. (4.5) and (4.6) are similar to those for the same system in the absence of microwave biases. An exact correspondence can be made by introducing the quanti-

ties $\delta_1'=\delta_1+\phi_{01}$, $\delta_2'=\delta_2+\phi_{02}+n\theta$, and $I_{ci}'=I_{ci}J_n(2eI_{mi}/\hbar c_i\omega_i)$ for each $i=1,2$. Then, Eqs. (4.5) and (4.6) become

$$\frac{\hbar c_1}{2e}\ddot{\delta}_1'+\frac{\hbar}{2eR_1}\dot{\delta}_1'+I_{c1}'\sin\delta_1' =\Delta I_{01}+\frac{\hbar}{2eL}(\delta_2'-\delta_1')-\frac{\hbar}{2eL}\Delta\delta'(0)+I_{N1}\ , \quad (4.9)$$

$$\frac{\hbar c_2}{2e}\ddot{\delta}_2'+\frac{\hbar}{2eR_2}\dot{\delta}_2'+I_{c2}'\sin\delta_2' =\Delta I_{02}+\frac{\hbar}{2eL}(\delta_1'-\delta_2')-\frac{\hbar}{2eL}\Delta\delta'(0)+I_{N2}\ , \quad (4.10)$$

Now we write Eqs. (4.9) and (4.10) in the form of the two-dimensional Langevin equation. That is,

$$\frac{\partial}{\partial t}\begin{bmatrix}\dot{\delta}_1\\ \dot{\delta}_2\end{bmatrix}=\begin{bmatrix}-\frac{1}{R_1c_1}\dot{\delta}_1\\ -\frac{1}{R_2c_2}\dot{\delta}_2\end{bmatrix}+\begin{bmatrix}-\xi_1\sin\delta_1'+\zeta_1(\delta_2'-\delta_1')+\chi_1\\ -\xi_2\sin\delta_2'+\zeta_2(\delta_1'-\delta_2')+\chi_2\end{bmatrix} +x(t)\begin{bmatrix}\gamma_1\\ \gamma_2\end{bmatrix}, \quad (4.11)$$

with

$$\langle x(t_1)x(t_2)\rangle=\delta(t_1-t_2)\ ,$$

where

$$\xi_i=\frac{2eI_{ci}}{\hbar c_i},\quad \zeta_i=\frac{1}{Lc_i},\quad \text{and}\quad \chi_i=\frac{2e\Delta I_{0i}}{\hbar c_i}\mp\frac{\Delta\delta(0)}{Lc_i}$$

for $i=1,2$. According to Eq. (4.1), γ_1 and γ_2 have the relations

$$\gamma_1=\frac{2e}{\hbar c_1}\left[\frac{n\hbar\nu_1}{2R_1}\coth\left(\frac{n\hbar\nu_1}{4kT}\right)\right]^{1/2}, \quad (4.12)$$

$$\gamma_2=\frac{2e}{\hbar c_2}\left[\frac{n\hbar\nu_2}{2R_2}\coth\left(\frac{n\hbar\nu_2}{4kT}\right)\right]^{1/2}. \quad (4.13)$$

From Eqs. (4.11) to (4.13) one can get a good physical picture of this system by considering the mechanical analogy where two particles with masses $m_1=\hbar c_1/2e$ and $m_2=\hbar c_2/2e$ are moving down two wavy slopes and coupled by a spring with a coupling constant $1/L$, as illustrated in Fig. 3. The equations of motion describe two particles undergoing Brownian motion with coefficients of viscosity $\hbar/2eR_1$ and $\hbar/2eR_2$, respectively. The normalized potentials of the two particles are given by

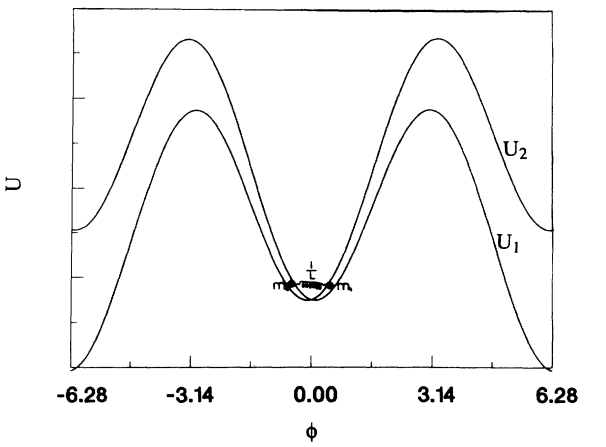

FIG. 3. The mechanical analogy of the readout system for both junctions locked on quantized voltage step.

$$U_1(\delta_1',\delta_2')=-\chi_1\delta_1'-\xi_1\cos\delta_1'+\frac{\zeta_1}{2}(\delta_1'-\delta_2')^2+C_1\ , \quad (4.14)$$

and

$$U_2(\delta_1',\delta_2')=-\chi_2\delta_2'-\xi_2\cos\delta_2'+\frac{\zeta_2}{2}(\delta_2'-\delta_1')^2+C_2\ , \quad (4.15)$$

where C_1 and C_2 are the trivial potential constants. The average slopes represent the parameter χ_i for $i=1,2$, and they are proportional to the current differences from the centers of the constant voltage steps, respectively. Provided the noise is Gaussian and white, it is straightforward to obtain the corresponding Fokker-Planck equation

$$\frac{\partial P(\dot{\delta}_1',\delta_1',\dot{\delta}_2',\delta_2')}{\partial t}=-\dot{\delta}_1'\frac{\partial P}{\partial\delta_1'}-\dot{\delta}_2'\frac{\partial P}{\partial\delta_2'}-[(-\xi_1\sin\delta_1'+\chi_1+\zeta_1(\delta_2'-\delta_1')]\frac{\partial P}{\partial\dot{\delta}_1'}+\frac{\partial}{\partial\dot{\delta}_1'}\left[\frac{\dot{\delta}_1'P}{R_1c_1}\right] -[-(\xi_2\sin\delta_2'+\chi_2+\zeta_2(\delta_1'-\delta_2')]\frac{\partial P}{\partial\dot{\delta}_2'}+\frac{\partial}{\partial\dot{\delta}_2'}\left[\frac{\dot{\delta}_2'P}{R_2c_2}\right]+\gamma_1^2\frac{\partial^2P}{\partial\dot{\delta}_1'^2}+\gamma_2^2\frac{\partial^2P}{\partial\dot{\delta}_2'^2}\ , \quad (4.16)$$

where P is the probability distribution. In general, Eq. (4.16) cannot be solved analytically. However, the real experimental situation we are interested in could further simplify the equation. Since, in general, the inductance L (in the range μH–nH) between two hysteretic junctions is at least 1000 times larger than the Josephson inductance $L_{Ji}=\hbar/2eI_{ci}$ (in the range pH–10 fH), therefore, $\xi_i=1/c_iL_{Ji}\gg\zeta_i=1/Lc_i$; and the contribution to the differential equation from the ζ_i terms is at least 1000 times less than that of the ξ_i terms. It is a good approximation to neglect those coupling terms with ζ_i. Note that when the Josephson inductance L_{Ji} is compatible with the coupling inductance L, the two biasing microwave frequencies will interfere with one another. The analysis of phase lock on the individual biasing frequency in Sec. II is no longer true. Since we have assumed that the Josephson inductance L_{Ji} is much less than the coupling inductance L according to the realistic situation,

the noise analysis in this section should be consistent with the analysis in Sec. II. Thus Eq. (4.16) can be decoupled into two independent Fokker-Planck equations; namely,

$$\frac{\partial P(\dot{\delta}_i',\delta_i')}{\partial t}=-\dot{\delta}_i'\frac{\partial P}{\partial \delta_i'}-(-\xi_i\sin\delta_i'+\chi_i)\frac{\partial P}{\partial \dot{\delta}_i'}+\frac{\partial}{\partial \dot{\delta}_i'}\left[\frac{\dot{\delta}_i' P}{R_i c_i}\right]+\gamma_i^2\frac{\partial^2 P}{\partial \dot{\delta}_i'^2} \tag{4.17}$$

for $i=1$ and 2. Equation (4.17) has the same form of the Fokker-Planck equation for an individual junction. The Fokker-Planck equation for a single junction has been studied by a number of authors [10,18–20]. The more general treatment for different junction parameters was given by Biswas and Jha [10]. In their approach, the basic assumptions are that the phases of both junctions spend most of their time in the relative minimum, and it is almost everywhere in equilibrium. For this situation the deviation currents from the centers of the two constant-voltage steps must be less than the critical current, and the ambient temperature should be far enough below the transition temperature of the superconductor so that the diffusion of the particles occurs only within the troughs. By applying Biswas and Jhas' result, the voltage roundoffs from $nh\nu_1/2e$ and $nh\nu_2/2e$ are

$$\langle \delta V_{ni}\rangle=\frac{\hbar}{2eR_i c_i}\left[\left[1+\frac{8eI_{ci}'R_i^2 c_i}{\hbar}[1-(\Delta I_{ci}/I_{ci}')^2]^{1/2}\right]^{1/2}-1\right]\times\exp\left\{\frac{8eI_{ci}'}{\hbar R_i c_i^2\gamma_i^2}\left[[1-(\Delta I_{ci}/I_{ci}')^2]^{1/2}+\frac{\Delta I_{ci}}{I_{ci}'}\sin^{-1}\left[\frac{\Delta I_{ci}}{I_{ci}'}\right]\right]\right\}\sinh\left[\frac{4\pi e\Delta I_{ci}}{\hbar R_i c_i^2\gamma_i^2}\right] \tag{4.18}$$

for $i=1,2$. The magnetic flux created by the deviation of the junction voltages is

$$\Delta\phi=\frac{\hbar}{2e}\int_0^t(\langle\delta V_{n1}\rangle+\langle\delta V_{n2}\rangle)dt\ . \tag{4.19}$$

In Eq. (4.18) the voltage roundoff is written as a function of current deviation from the center of a constant step. Suppose that both dc bias currents can be locked on the centers of each constant-voltage step by a feedback loop to keep the total current flowing through each individual junction constant (see, for example, Fig. 4). The uncertainty of the voltage difference is limited by the fluctuations of the feedback bias current, that is,

$$\delta V(\Delta I_{01},\Delta I_{02})=\langle\delta V_{n1}(\Delta I_{01})\rangle+\langle\delta V_{n2}(\Delta I_{02})\rangle\ . \tag{4.20}$$

In Fig. 4 we plot the logarithm of the voltage uncertainty δV versus the bias fluctuation $\Delta I=\Delta I_{01}=\Delta I_{02}$ from $\Delta I=0.005I_{ci}'$ to $\Delta I=0.995I_{ci}'$ with junction parameters $R_1=R_2=40\ \Omega$, $c_1=c_2=35$ pF, and $I_{c1}'=I_{c2}'=100\ \mu$A, and the voltage of the junction at about 1 mV at a temperature $T=4$ K. Notice that the uncertainty of the differential voltage due to thermal noise in the junctions is so tiny that even though the bias current fluctuates near the critical current of the phase-locked state the fluctuation of the differential voltage is only tens of μV. Nevertheless, if the bias current is near the critical current, the phase-locked state becomes unstable and phase slip occurs easily. With the scheme illustrated in Fig. 5, if we can control the current fluctuation to within 0.5 μA, then in the same situation the fluctuation of the differential voltage is less than 10^{-300} V which is completely negligible.

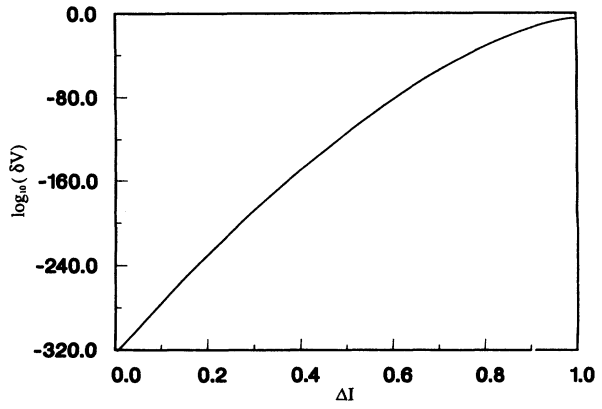

FIG. 4. The voltage uncertainty (in volts) vs the current deviation (in unit of induced current amplitude) for junction parameters $c_1=c_2=35$ pF, $R_1=R_2=40\ \Omega$, and $I_{c1}'=I_{c2}'=100\ \mu$A with junction voltage 1 mV and a voltage difference of 1 μV between the two junctions at temperature $T=4$ K.

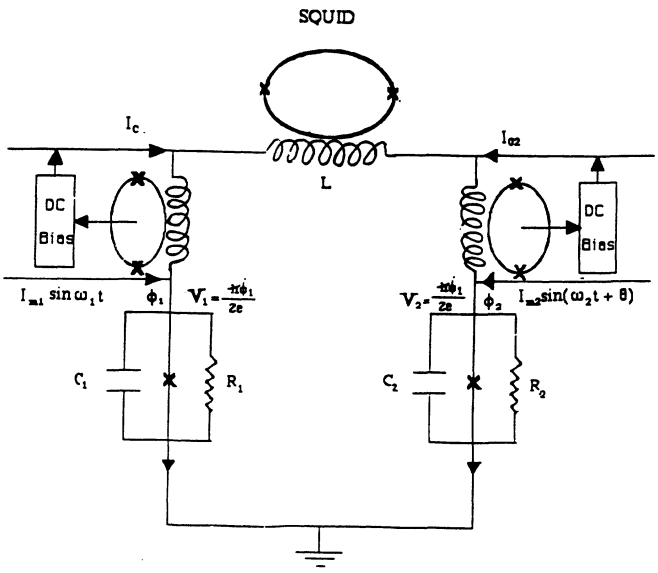

FIG. 5. The scheme for constant current bias mode.

Another experimental realization of this scheme is to operate with fixed external dc biases. From Eqs. (4.7) and (4.8), we see that the dc current flowing through each junction depends on the microwave frequency difference. If the frequency difference is time dependent the current deviation from the center of the quantized voltage state is also time dependent. Thus the deviation of the differential voltage is a function of the differential voltage itself. With regard to the accuracy required by experiments, one may set the maximum allowable current in response to the differential frequency signal according to the similar result shown in Fig. 5. Also, we note that the maximum allowable current should not be too close to the critical current of the phase-locked step since the junctions become more vulnerable to external disturbance and more easily lose their phase-locked state.

V. SUMMARY AND CONCLUSION

We have proposed that the scheme used in the comparison of two hysteretic Josephson junctions can be applied as an ultrahigh accuracy differential frequency readout at millimeter wavelengths. An important feature of this scheme is that since the ac Josephson relation $V=nh\nu/2e$ is independent of the microwave power, the differential frequency readout is insensitive to the photon fluctuation of the biased microwaves which occurs in conventional photon-detection schemes. Any fluctuation of microwave power affects only the critical current of the quantized voltage step, Eqs. (2.12) and (2.13). If one biases the two junctions to the centers of the quantized steps, and if the critical current is large enough, then such fluctuations are not important. In Eq. (2.15) we notice that the resolution of the differential frequency is proportional to $(\Delta t)^{3/2}$ where Δt is the measurement time period. Therefore, if the signal of the differential frequency between two sources is a monotonic signal (dc signal) for a longer period than the measurement time, an unprecedented measurement may be achieved. For example, the experiment by Jain, Luken, and Tsai [1] is capable of measuring the earth's gravitation redshift on two Josephson junctions separated in height by 7.2 cm, over a ten-hour period of measurement time.

The implication of the previous experiments [1,3–5] for the Josephson junction comparisons has been addressed. Any deviation from the ac Josephson relation can be observed in this scheme according to the Stewart-McCumber model. The phase rigidity of the superconducting coil between two Josephson junctions does not induce the phase locking between the two junctions since the magnetic flux inside the superconducting inductor responds to the phase change of the two junctions.

The stability of this scheme has been considered. The inductance between the two junctions does not degrade the stability of the two independent junctions. In fact, when the inductance between them is less than the Josephson inductance of each junction, the stability would increase dramatically. This effect could be applied to stabilize the voltage standard, especially the high voltage standard. We plan to address this point elsewhere [31].

The effect of thermal noise on the Josephson junctions in this measurement scheme is discussed. The Langevin and the Fokker-Planck equations for this scheme have been derived. When the inductance between the two junctions is larger than the Josephson inductance in each one of the junctions, the Fokker-Planck equation can be decoupled into two independent sets of Fokker-Planck equations, each having the same form as that of a single junction. By applying the previous analysis for a single junction by Biswas and Jha [10], we obtain the voltage roundoff effect for both junctions. For the case of a fixed junction current (varying the external dc bias current of each function in response to the signal of the differential frequency), the uncertainty of the differential voltage is a function of the fluctuation of the beedback bias current. For the case of a fixed external dc bias current, the deviation from the idea response to the differential frequency signal is also a function of the signal itself. However, as illustrated in Fig. 4, the deviation from the intrinsic thermal noise in the two hysteretic junctions of this readout system is not significant.

The Josephson junctions we consider here are the same as those used in a large array voltage standard. Since in this array the distance between two adjacent Josephson junctions is more than 10 μm, the interaction between two adjacent junctions is negligible [32]. We can thus consider each of the junctions in the array independently. Also, due to the large overlap of the center of adjacent steps in a hysteretic junction, the Josephson-junction array can be biased by a single dc current, and the microwave-induced amplitude of the current step is the smallest induced critical current of one of the series junctions. The total voltage of this array is the sum of the voltages of all junctions. The voltage for present existing arrays can be biased up to 12 V and the phase-locked quantum number is as high as 60 000 [33]. Since the thermal intrinsic noise of a single junction in the series-array voltage standard is so small, the total thermal noise in the series array does not contribute to the measurement uncertainty significantly. Thus we would expect that the signal-to-noise ratio will improve by using two large arrays in the readout system.

In conclusion, this proposed differential frequency readout system at millimeter wavelength has been theoretically shown to achieve an ultrahigh accuracy. Possible applications of this active-interferometer-readout system include experiments for testing general relativity. The fundamental limitation on active interferometer schemes is the phase diffusion of the two uncorrelated lasing modes which bias the junctions. A laser system [so-called correlated spontaneous emission laser (CEL)] has been proposed [34] and tested [35]. In this laser system the diffusion of the relative phase of two lasing modes can be quenched by level coherence of the laser transitions. By combining these systems, e.g., CEL and Josephson-junction readout system, a dramatic improvement on the precision of measurement is expected. From the experimental side, Josephson-junction series arrays containing 2076, 3020, and 18 992 junctions have been developed and are readily available. However, an active interferometer near 100 GHz utilizing a CEL mechanism still needs to be developed.

ACKNOWLEDGMENTS

We thank Robert Giannelli for careful reading and suggestions for this manuscript. This work has been supported by the United States Department of Energy through Contract No. DE-AC04-76-DP00789, and through the Sandia-University Research Program.

[1] A. K. Jain, J. E. Lukens, and J.-S. Tsai, Phys. Rev. Lett. **58**, 1165 (1987).
[2] W. C. Stewart, Appl. Phys. Lett. **12**, 277 (1968); D. E. McCumber, J. Appl. Phys. **39**, 3113 (1968).
[3] J. Clarke, Phys. Rev. Lett. **21**, 1566 (1968).
[4] T. Dan Bracken and W. O. Hamilton, Phys. Rev. B **6**, 2603 (1972).
[5] J. C. Macfarlane, Appl. Phys. Lett. **22**, 549 (1973).
[6] Jaw-Shen Tsai, A. K. Jain, and J. E. Lukens, Phys. Rev. Lett. **51**, 316 (1983).
[7] D. G. McDonald, Science **247**, 177 (1990).
[8] L. Z. Wang and Robert V. Duncan (unpublished).
[9] *Experimental Gravitation and Measurement Theory,* edited by P. Meystre and M. O. Scully (Plenum, New York, 1983).
[10] A. C. Biswas and S. S. Jha, Phys. Rev. B **2**, 2543 (1970).
[11] R. L. Kautz, J. Appl. Phys. **52**, 3528 (1981).
[12] R. L. Kautz, C. A. Hamilton, and F. L. Lloyd, IEEE Trans. Magn. **Mag-23**, 883 (1987).
[13] K. Nordtvedt, Phys. Rev. B **1**, 81 (1970).
[14] R. H. Koch, Bull. Am. Phys. Soc. **28**, 570 (1983).
[15] F. Bloch, Phys. Rev. B **7**, 981 (1970).
[16] T. A. Fulton, Phys. Rev. B **7**, 109 (1970).
[17] R. L. Kautz, J. Appl. Phys. **62**, 198 (1987).
[18] M. J. Stephen, Phys. Rev. **182**, 531 (1969).
[19] P. A. Lee, J. Appl. Phys. **42**, 325 (1971).
[20] V. Ambegaokar and B. I. Halperin, Phys. Rev. Lett. **22**, 1364 (1969).
[21] W. H. Henkels and W. W. Webb, Phys. Rev. Lett. **26**, 1164 (1971).
[22] T. A. Fulton and L. N. Dunkleberger, Phys. Rev. B **9**, 4760 (1974).
[23] B. A. Fluberman, J. P. Crutchfield, and N. H. Packard, Appl. Phys. Lett. **37**, 750 (1980).
[24] R. F. Miracky, J. Clarke, and R. H. Koch, Phys. Rev. Lett. **50**, 856 (1983).
[25] M. Octavio, Phys. Rev. B **29**, 1231 (1984).
[26] N. F. Pedersen and A. Davidson, Appl. Phys. Lett. **39**, 830 (1981).
[27] E. G. Gwinn and R. M. Westervelt, Phys. Rev. Lett. **54**, 1613 (1985).
[28] M. J. Kajaito and M. M. Salomaa, Solid State Commun. **53**, 99 (1985).
[29] M. Iansiti, Qing Hu, R. M. Westervelt, and M. Tinkham, Phys. Rev. Lett. **55**, 746 (1985).
[30] D. Rogovin and D. J. Scalapino, Ann. Phys. (N.Y.) **86**, 1 (1974).
[31] L. Z. Wang and Robert V. Duncan (unpublished).
[32] D. W. Jillie, J. E. Lukens, and Y. H. Kao, Phys. Rev. Lett. **38**, 915 (1977).
[33] A. Hamilton, F. L. Lloyd, K. Chieh, and W. C. Goeke, IEEE Trans. Instrum. Meas. **IM-38**, 314 (1989).
[34] M. O. Scully, Phys. Rev. Lett. **55**, 2802 (1985).
[35] Michael P. Winters, John L. Hall, and Peter E. Toschek, Phys. Rev. Lett. **65**, 3116 (1990).